SUPPORTING INFORMATION

Atmospheric impact of 2-methylpentanal emissions: Kinetics, photochemistry, and formation of secondary pollutants

María Asensio[1,2], Sergio Blázquez[1,2,#], María Antiñolo[1,2], José Albaladejo[1,2], Elena Jiménez[1,2,*]

[1]Instituto de Investigación en Combustión y Contaminación Atmosférica, Universidad de Castilla-La Mancha, Camino de Moledores s/n, Ciudad Real, 13071, Spain
[2]Departamento de Química Física, Universidad de Castilla-La Mancha, Avda. Camilo José Cela 1B, Ciudad Real, 13071, Spain

Correspondence to: Elena Jiménez (elena.jimenez@uclm.es)

[#] Current address. Escuela Técnica Superior de Ingenieros Industriales, Departamento de Química Física, Universidad de Castilla-La Mancha, Avda. España s/n, Albacete, 02071, Spain.

I. ADDITIONAL INFORMATION ON MATERIALS AND METHODS

Gas-phase UV spectroscopy (220-360 nm)

To obtain reliable values of the UV absorption cross section (σ_λ in cm^2 $molecule^{-1}$) several UV spectra were recorded in a cylindrical jacketed gas cell (optical path length, l = 107.15 cm) using different concentrations of 2MP (1.02 – 9.65 Torr). The temperature inside the cell was maintained at (298 ± 1) K by flowing water from a thermostatic bath (Huber, Polystat cc1) through the jacket. According to the Beer-Lambert's law (Eq. **ES1**) σ_λ was obtained from the slope of the measured absorbance (A_λ) *versus* [2MP] plots.

$$A_\lambda = \sigma_\lambda \, l \, [2MP] \qquad \text{(ES1)}$$

Some of these plots at several wavelengths are depicted in **Fig. S1**, including the absorption maximum at 296 nm.

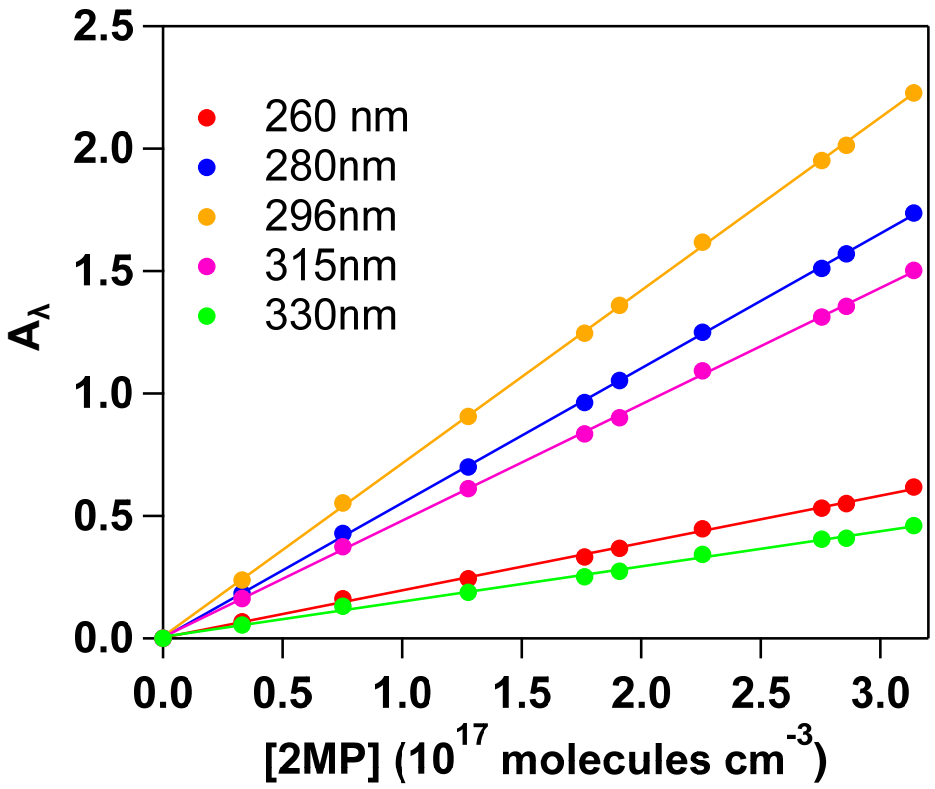

Figure S1. Examples of plots of Beer-Lambert's law for 2MP at room temperature.

UV photodissociation of 2MP

A 20-cm cylindrical jacketed cell was filled with (760 ± 2) Torr of diluted 2MP in synthetic air (dilution factors, $P_{2MP}/(P_{2MP}+P_{air})$, ranged from 1.07 to 1.73 × 10^{-3}). The temperature of the gas mixture was maintained at (298 ± 1) K by recirculating water through the jacket from a thermostatic bath (CD-200F, CORIO). The mixture was irradiated with a solar simulator (model 11002-2, SunLite^{TM}) at λ > 290 nm during 30, 60, 90, 120, or 150 min. Average irradiance was (2.335 ± 0.126) Suns. One Sun is the irradiance of the AM1.5G reference solar spectrum (Gueymard et al., 2002). The initial concentration of 2MP in the photolysis cell ranged from 1.12 to 6.55 × 10^{16} molecules cm^{-3}. Gas-phase species in the cell were monitored by FTIR. At each photolysis time, the gas mixture (unreacted 2MP and reaction products) was transferred to a 16-L White-type cell, with an optical path length of 71 m, coupled to a FTIR spectrometer (Nicolet Nexus 870, Thermo Fisher Scientific) (Asensio et al., 2022) with a resolution of 2 cm^{-1}. Spectra were recorded between 650 and 4000 cm^{-1} and after the accumulation of 32 interferograms. The selected IR bands for monitoring 2MP were those centered at 1748 cm^{-1} and between 2630 and 3000 cm^{-1}.

Smog chamber experiments. Kinetics and product study

The 16-L gas cell and a 264-L chamber were surrounded by actinic lamps (Philips Actinic BL TL 40W/10 1SL/25, λ = 340-400 nm) (Ballesteros et al., 2017; Antiñolo et al., 2019) to generate Cl atoms *in situ* by photolysis of Cl_2. The 264-L chamber was also surrounded by 4 germicidal lamps (Philips TUV 36W SLV/6, λ=254 nm) to generate OH radicals by H_2O_2 photolysis. Gas-phase species were introduced in the chambers from a gas line with two capacitor pressure transducers (Leybold, model Ceravac, 10 and 1000 Torr full scale) and the species were diluted with synthetic air at (298±2) K and (760±5) Torr of total pressure. Coupled to the chambers and depending on the experiment performed, specific instrumentation was used to monitor the time evolution of species:

In the **relative kinetic experiments**, IR spectra were recorded every 2 min and the IR bands selected for monitoring 2MP, isoprene, and propene were 2630-3000 cm^{-1}, 3100 cm^{-1}, and 3050-3100 cm^{-1}, respectively. Ranges of initial concentrations were $[2MP]_0$ = (3.7 - 9.4) × 10^{14} molecules cm^{-3}, $[isoprene]_0$ = (3.7 - 6.2) × 10^{14} molecules cm^{-3} or $[propene]_0$ = (4.2 - 6.2) × 10^{14} molecules cm^{-3}, and $[Cl_2]_0$ = (3.4 - 4.2) × 10^{14} molecules cm^{-3}.

Preliminary experiments on the loss processes of 2MP and reference compounds in the absence of Cl atoms were done as described in previous studies (Antiñolo et al., 2019; Antiñolo et al., 2020):

- *Wall losses*: in the absence of Cl_2 and UV light (k_w)
- *Reaction with Cl_2*: in the absence of UV light (k'_{Cl_2})
- *UV photolysis*: irradiating the sample in the absence of Cl_2 (k_{hv})

As shown in **Table S1**, all species exhibited wall losses and no photolysis at the emission wavelengths of the actinic lamps (λ = 340-400 nm). The latter observations are in agreement with the very low absorption of 2MP in that range observed in the present work and for the reference alkenes.

Table S1. Average loss rate coefficients due to different processes observed for the 2MP and the reference compounds.

Compound	k_w (10^{-5} s^{-1})	$k_{h\nu}$ (10^{-5} s^{-1})	k'_{Cl_2} (10^{-5} s^{-1})	k_{Total_loss} (10^{-5} s^{-1})
2MP	1.22±0.15	-	-	**1.22±0.15**
Propene	1.20±0.31	-	-	**1.20±0.31**
Isoprene	0.63±0.23	-	0.77±0.33	**1.41±0.41**

In the **product studies**, a GC-MS (Thermo Electron, models Trace GC Ultra and DSQ II) equipped with a BPX35 column (30 m × 0.25 mm ID × 0.25 µm, SGE Analytical Science) was used (Asensio et al., 2022). The solid-phase microextraction (SPME) technique was used as sampling method with a 50/30 µm divinylbenzene/carboxen/polydimethylsiloxane (DVB/CAR/PDMS) fiber (Supelco) exposed during 10 min to the gas mixture in the chamber. For the product study of the OH-reaction, 2MP/H_2O_2/air mixtures were irradiated for 70 min by the germicidal lamps, whereas in the Cl atoms experiments, 2MP/Cl_2/air mixtures were irradiated with the actinic lamps for 60 min. IR spectra, chromatograms and mass spectra were recorded every 2 min, 15 min and 20 s, respectively. For the PTR-ToF-MS experiments, concentrations were lower due to its high sensitivity. The mass spectra of the reactive gas mixture were recorded with a time resolution of 20 s and the detected mass range was set between 29 and 390.86 amu working at E/N = 138 Td and V_{drift} = 650V. Prior the *in situ* measurements, a calibration of the PTR-ToF-MS was made in the concentration range between 18 and 190 ppb. Preliminary tests were carried out to check if products were generated during the dark reaction of 2MP with the oxidant precursor and/or during the UV light exposure of 2MP.

Table S2. Initial concentrations used in the product study of reactions R2 and R3 according to the VOC detection technique.

Detection Technique	$[2MP]_0$ (10^{14} molecules cm^{-3})	$[H_2O_2]_0$ (10^{14} molecules cm^{-3}) [a]	$[Cl_2]_0$ (10^{14} molecules cm^{-3}) [a]
FTIR	6.1 - 8.5	-	1.6 - 5.4
	8.3 [b]	-	7.8 [b]
GC-MS	1.5 - 4.4	-	1.1 - 2.5
PTR-ToF-MS	0.13 - 0.23	3.8	0.11 - 0.14

[a] Estimated concentrations; [b] In SOA experiments

Pulsed Laser Photolysis-Laser Induced Fluorescence (PLP-LIF) technique

The temperature of the reactor was measured by a type K (chromel-alumel) thermocouple inserted a few millimeters above the reaction zone. The temperature was controlled (±0.2 K) by flowing water (for $T \geq 278$ K) or water/ethanol mixture (for $T \leq 268$ K) through the double wall of the reactor. The total pressure was controlled by means a needle valve placed between the exit of the reactor and the pump, and it was measured by a pressure transducer (Oerlikon Leybold Vacuum, model CERAVAC CTR 100, Full scales of 0–100 Torr and 0–1000 Torr). The total incoming gas flow (F_{Total}) consisted of a mixture of bath gas (F_{He} = 269.8–468.1 standard cubic centimeters per minute (sccm)), OH radical precursor ($F_{H_2O_2/He}$ =1.31–26.49 sccm) and different concentrations of diluted 2MP (F_{2MP} = 0.44–14.38 sccm), all of them controlled by calibrated mass flow controllers. The 2MP diluted mixtures were prepared in a 10 L storage bulb by introducing a specific pressure of pure 2MP and diluting it with He up to around 770 Torr. The dilution factor (*f*), calculated as the ratio of the pure 2MP pressure and total pressure in the storage bulb, was in the (1.37–6.65)×10^{-3} range. In **Table S3** are shown the experimental conditions employed.

The OH radicals were generated *in situ* from the PLP of H_2O_2 at 248 nm. This radiation was emitted by a KrF excimer laser (Coherent, Excistar 200), with a laser fluence of 23 mJ $pulse^{-1}$ cm^{-2} at 10 Hz. The OH radicals generated in electronic ground state were excited at *ca*. 282 nm to the first excited electronic state (laser energy 0.8–1.2 mJ $pulse^{-1}$ at 10 Hz) by the second harmonic of a Rhodamine-6G dye laser (LiopTech, LiopStar). The dye laser was pumped by the second harmonic of a Nd-YAG laser (InnoLas, SpitLight 1200). At 90 degrees from photolysis and excitation lasers, the laser induced fluorescence (LIF) at *ca*. 310 nm was collected by a filtered phototube (Thorn EMI, 9813B). The LIF signal (I_{LIF}) was integrated by a boxcar unit and treated by computer software (Stanford Research Systems, SR270). By varying the delay between excitation and photolysis lasers, the time evolution of I_{LIF} was obtained. Under *pseudo*-first order conditions, *i.e*. when initial concentration of 2MP is in large excess with respect to that of OH radicals, the time evolution of I_{LIF} follows a single exponential decay:

$$I_{LIF} = I_{LIF,0} \exp(-k't) \quad \text{(ES2)}$$

where $I_{LIF,0}$ is the LIF intensity at time 0 and k' is the *pseudo*-first order rate coefficient for a given 2MP concentration, temperature, and pressure. Some examples of temporal evolution of I_{LIF} are shown in **Figure S2**. k' includes all OH-loss processes: reaction with 2MP and H_2O_2, and diffusion out from the detection zone mainly.

$$OH + 2MP \rightarrow Products \quad \text{(RS1)}$$

$$OH + H_2O_2 \rightarrow H_2O + HO_2 \quad \text{(RS2)}$$

$$OH \rightarrow Other\ losses \quad \text{(RS3)}$$

From the analysis of k' in presence and absence (k'_0) of 2MP, the second-order rate coefficient $k_{OH}(T)$ at a given temperature is obtained.

$$k' - k'_0 = k_{OH}(T)[2MP]_0 \quad \text{(ES3)}$$

The concentration of 2MP in the reactor was calculated as follows:

$$[2MP]_0 = 3.24 \times 10^{16} \text{molecules cm}^{-3} Torr^{-1} \frac{F_{2MP}}{F_T} f P_T(Torr) \frac{298\ \text{K}}{T\ (\text{K})} \quad \text{(ES4)}$$

From the slope of $k'–k'_0$ *versus* $[2MP]_0$, $k_{OH}(T)$ was determined at each temperature and pressure.

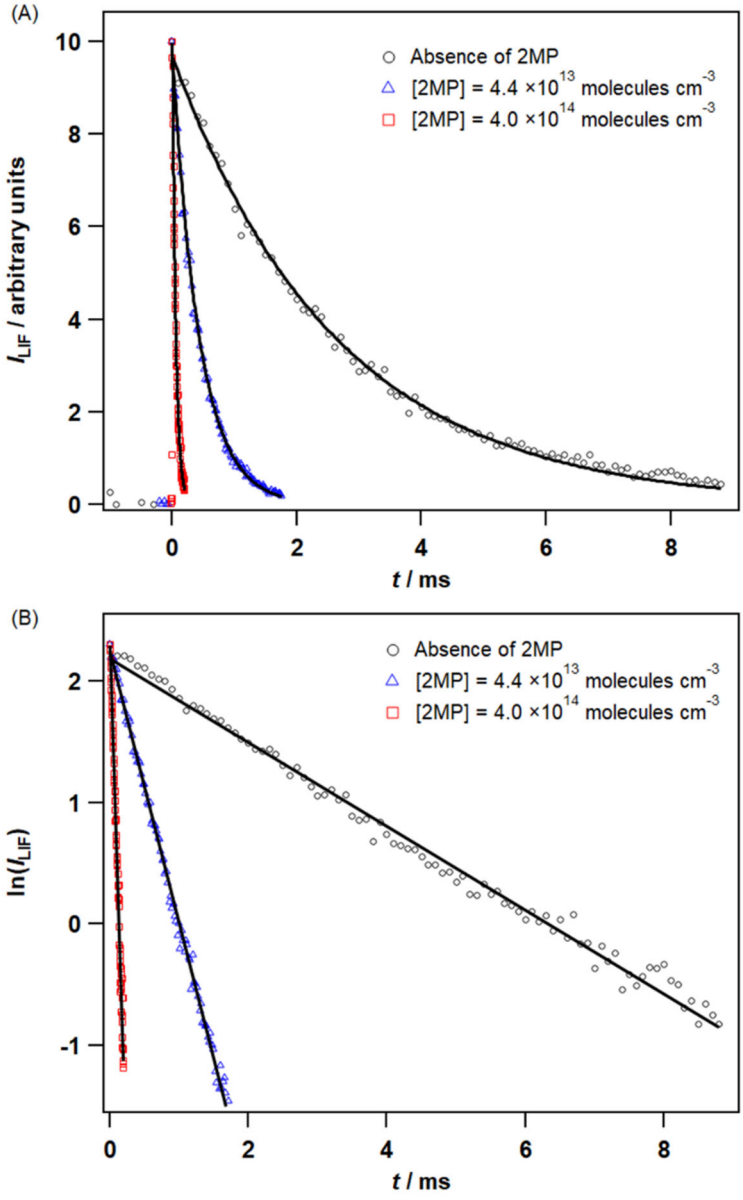

Figure S2. Temporal profiles of I_{LIF} from OH radicals in the absence and presence of 2MP at 263 K and 50 Torr.

Table S3. Experimental conditions employed and *pseudo*-first order coefficient (corrected with k_0') obtained in the kinetic study of the OH + 2MP reaction.

T / K	P_T / Torr	f / 10^{-3}	F_{2MP} / sccm	$F_{H_2O_2/He}$ / sccm	F_{He} / sccm	$[2MP]_0$ / 10^{14} molecules cm^{-3}	k'-k'_0 / 10^3 s^{-1}
263	50	6.646	0.92 – 8.61	4.03	275.3 – 283.6	0.44 – 3.56	1.75 – 15.58
	50	6.646	0.92 – 9.57	4.03	274.4 – 283.6	0.44 – 3.96	1.88 – 16.97
	250	2.771	0.92 – 6.69	26.49	254.1 – 260.5	0.95 – 5.91	3.51 – 24.95
	250	2.771	0.92 – 6.69	26.49	254.1 – 260.5	0.95 – 5.91	3.52 – 24.93
	500	2.771	0.44 – 3.81	26.49	349.1 – 352.8	0.82 – 5.19	2.88 – 22.59
	500	2.771	0.44 – 3.81	26.49	349.1 – 352.8	0.82 – 5.19	2.60 – 21.72
268	50	6.646	0.92 – 9.57	4.03	274.4 – 283.6	0.43 – 3.88	1.66 – 16.09
	50	6.646	0.92 – 9.57	4.03	274.4 – 283.6	0.43 – 3.88	1.42 – 16.02
278	50	6.646	0.92 – 9.57	4.03	274.4 – 283.6	0.42 – 3.74	1.33 – 14.53
	50	6.646	0.92 – 9.57	4.03	274.4 – 283.6	0.42 – 3.74	1.53 – 14.54
288	50	6.646	0.92 – 9.57	4.03	274.4 – 283.6	0.40 – 3.61	1.34 – 13.13
	50	6.646	0.92 – 9.57	4.03	274.4 – 283.6	0.40 – 3.61	1.02 – 13.02
298	50	6.646	0.92 – 9.57	4.03	274.4 – 283.6	0.39 – 3.49	0.73 – 11.70
	50	6.646	0.92 – 9.57	4.03	274.4 – 283.6	0.39 – 3.49	1.16 – 11.92
	250	1.372	0.92 – 9.57	8.56	269.8 – 279.0	0.42 – 3.72	1.03 – 11.92
	250	2.771	0.92 – 7.65	8.56	456.1 – 463.5	0.51 – 3.62	1.19 – 11.94
	500	1.372	0.92 – 9.57	1.31	458.9 – 468.1	0.51 – 4.55	1.97 – 14.39
	500	2.771	0.44 – 3.81	26.49	349.1 – 352.8	0.72 – 4.58	1.92 – 14.82
309	50	2.771	1.88 – 14.38	4.03	269.8 – 283.6	0.30 – 2.13	0.92 – 6.83
	50	6.646	0.92 – 9.57	4.03	274.4 – 283.6	0.37 – 3.37	0.90 – 10.53
323	50	6.646	0.92 – 9.57	4.03	274.4 – 283.6	0.36 – 3.22	0.98 – 9.82
	50	6.646	0.92 – 9.57	4.03	274.4 – 283.6	0.36 – 3.22	0.85 – 9.46
338	50	6.646	0.92 – 9.57	4.03	274.4 – 286.6	0.34 – 3.08	0.93 – 8.62
	50	6.646	0.92 – 9.57	4.03	274.4 – 283.6	0.34 – 3.08	0.84 – 8.56
353	50	6.646	0.92 – 9.57	4.03	274.4 – 283.6	0.33 – 2.95	0.87 – 8.05
	50	6.646	0.92 – 9.57	4.03	274.4 – 283.6	0.33 – 2.95	0.88 – 8.22
	250	2.771	0.92 – 9.57	8.56	362.0 – 371.2	0.54 – 4.72	1.53 – 12.80
	250	2.771	0.92 – 9.57	8.56	362.0 – 371.2	0.54 – 4.72	1.33 – 12.62
	500	2.771	0.44 – 4.77	26.49	348.2 – 352.8	0.61 – 4.80	1.50 – 12.94
	500	2.771	0.44 – 4.77	26.49	348.2 – 352.8	0.61 – 4.80	1.66 – 12.95

II. ADDITIONAL RESULTS

UV photochemistry of 2MP

Table S4. Average UV absorption cross sections of 2MP (in base *e*) in the range of 220-360 nm at 1 nm intervals. Uncertainties are ± 2σ of the average.

λ (nm)	σ_λ (10^{-20} cm^2 molecule^{-1})	λ (nm)	σ_λ (10^{-20} cm^2 molecule^{-1})	λ (nm)	σ_λ (10^{-20} cm^2 molecule^{-1})
220	0.31 ± 0.10	267	2.85 ± 0.07	314	4.64 ± 0.10
221	0.30 ± 0.10	268	3.02 ± 0.08	315	4.46 ± 0.11
222	0.28 ± 0.10	269	3.20 ± 0.10	316	4.25 ± 0.11
223	0.27 ± 0.10	270	3.38 ± 0.11	317	3.99 ± 0.10
224	0.26 ± 0.11	271	3.56 ± 0.10	318	3.71 ± 0.11
225	0.24 ± 0.10	272	3.73 ± 0.09	319	3.45 ± 0.14
226	0.21 ± 0.09	273	3.91 ± 0.09	320	3.23 ± 0.14
227	0.19 ± 0.07	274	4.07 ± 0.06	321	3.02 ± 0.11
228	0.18 ± 0.06	275	4.24 ± 0.05	322	2.83 ± 0.08
229	0.18 ± 0.10	276	4.42 ± 0.05	323	2.65 ± 0.11
230	0.18 ± 0.12	277	4.61 ± 0.06	324	2.47 ± 0.10
231	0.18 ± 0.09	278	4.80 ± 0.07	325	2.30 ± 0.11
232	0.19 ± 0.09	279	4.97 ± 0.07	326	2.13 ± 0.12
233	0.20 ± 0.11	280	5.14 ± 0.06	327	1.97 ± 0.11
234	0.21 ± 0.10	281	5.30 ± 0.09	328	1.79 ± 0.12
235	0.22 ± 0.09	282	5.44 ± 0.09	329	1.58 ± 0.11
236	0.24 ± 0.10	283	5.57 ± 0.07	330	1.39 ± 0.13
237	0.26 ± 0.11	284	5.71 ± 0.06	331	1.20 ± 0.15
238	0.28 ± 0.09	285	5.85 ± 0.06	332	1.05 ± 0.15
239	0.30 ± 0.08	286	5.99 ± 0.08	333	0.93 ± 0.16
240	0.34 ± 0.10	287	6.12 ± 0.10	334	0.82 ± 0.16
241	0.37 ± 0.10	288	6.23 ± 0.11	335	0.72 ± 0.15
242	0.40 ± 0.10	289	6.34 ± 0.12	336	0.63 ± 0.13
243	0.43 ± 0.09	290	6.41 ± 0.11	337	0.55 ± 0.13
244	0.47 ± 0.08	291	6.47 ± 0.09	338	0.49 ± 0.17
245	0.52 ± 0.08	292	6.51 ± 0.07	339	0.42 ± 0.14
246	0.57 ± 0.09	293	6.57 ± 0.07	340	0.36 ± 0.11
247	0.62 ± 0.09	294	6.62 ± 0.11	341	0.30 ± 0.11
248	0.68 ± 0.08	295	6.64 ± 0.11	342	0.26 ± 0.11
249	0.74 ± 0.09	296	6.64 ± 0.11	343	0.22 ± 0.13
250	0.81 ± 0.08	297	6.62 ± 0.08	344	0.17 ± 0.11
251	0.88 ± 0.08	298	6.59 ± 0.08	345	0.14 ± 0.10
252	0.97 ± 0.09	299	6.56 ± 0.09	346	0.12 ± 0.12
253	1.05 ± 0.09	300	6.52 ± 0.09	347	0.11 ± 0.14
254	1.14 ± 0.09	301	6.47 ± 0.07	348	0.10 ± 0.11
255	1.23 ± 0.08	302	6.40 ± 0.07	349	0.09 ± 0.10
256	1.33 ± 0.05	303	6.32 ± 0.11	350	0.09 ± 0.12
257	1.44 ± 0.05	304	6.24 ± 0.12	351	0.08 ± 0.11
258	1.56 ± 0.06	305	6.14 ± 0.12	352	0.08 ± 0.14
259	1.69 ± 0.09	306	5.98 ± 0.10	353	0.09 ± 0.17
260	1.81 ± 0.09	307	5.79 ± 0.09	354	0.07 ± 0.08
261	1.95 ± 0.08	308	5.60 ± 0.10	355	0.07 ± 0.06
262	2.09 ± 0.08	309	5.44 ± 0.09	356	0.06 ± 0.07
263	2.23 ± 0.08	310	5.29 ± 0.08	357	0.06 ± 0.07
264	2.38 ± 0.08	311	5.13 ± 0.08	358	0.08 ± 0.11
265	2.54 ± 0.09	312	4.98 ± 0.09	359	0.07 ± 0.10
266	2.69 ± 0.08	313	4.82 ± 0.10	360	0.07 ± 0.08

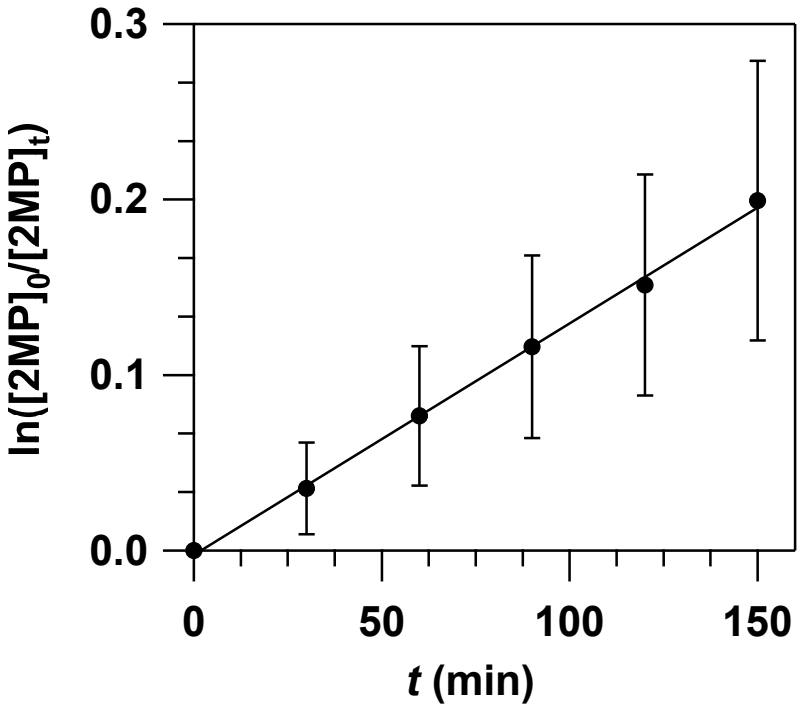

Figure S3. Plot of the 2MP loss after absorption of radiation at $\lambda \geq 290$ nm as a function of time.

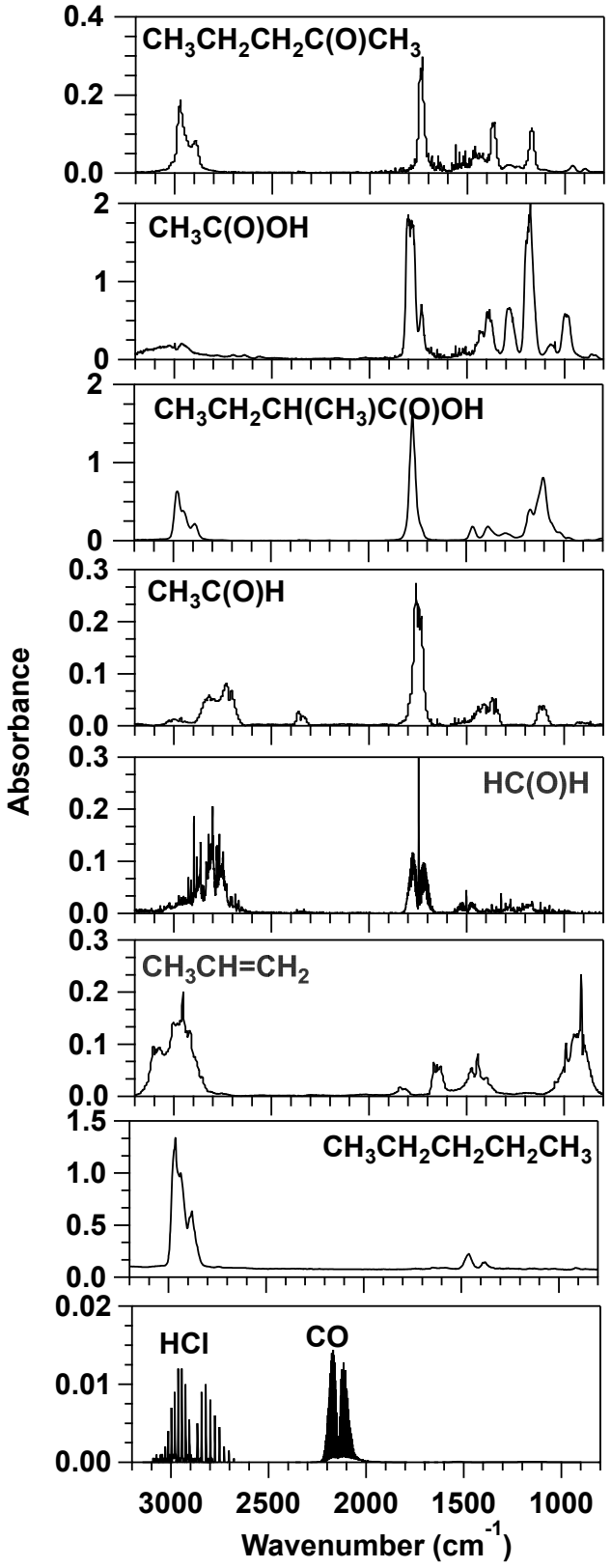

Figure S4. Reference infrared spectrum of 2-pentanone, acetic acid, acetaldehyde, formaldehyde, HCl and CO recorded in our lab. Pentane, 2-methylbutanoic acid, and propene spectra were taken from the NIST FTIR database.

Kinetics and products of Cl + 2MP reaction studied in smog chambers.

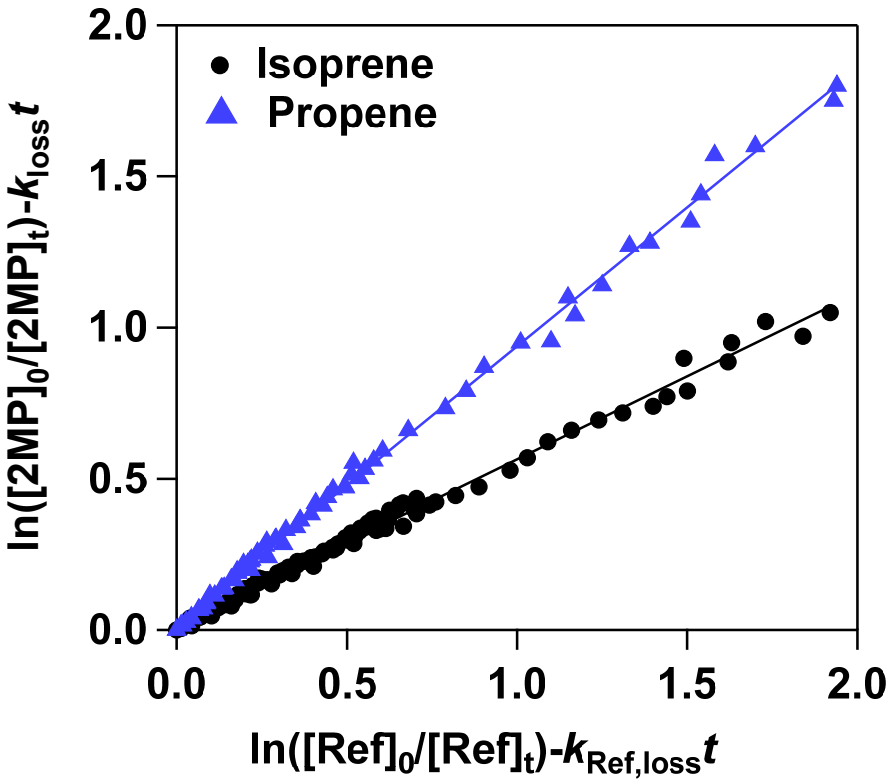

Figure S5. Plot of Equation (E2) for the Cl-reaction of 2MP using two reference compounds.

Detection by SPME/GC-MS: Gas chromatography coupled to mass spectrometry was also used in the product study of reactions R2 as an identification technique. In **Figure S6**, the recorded chromatograms before starting the Cl + 2MP reaction (a) and after 40 min (b) are shown.

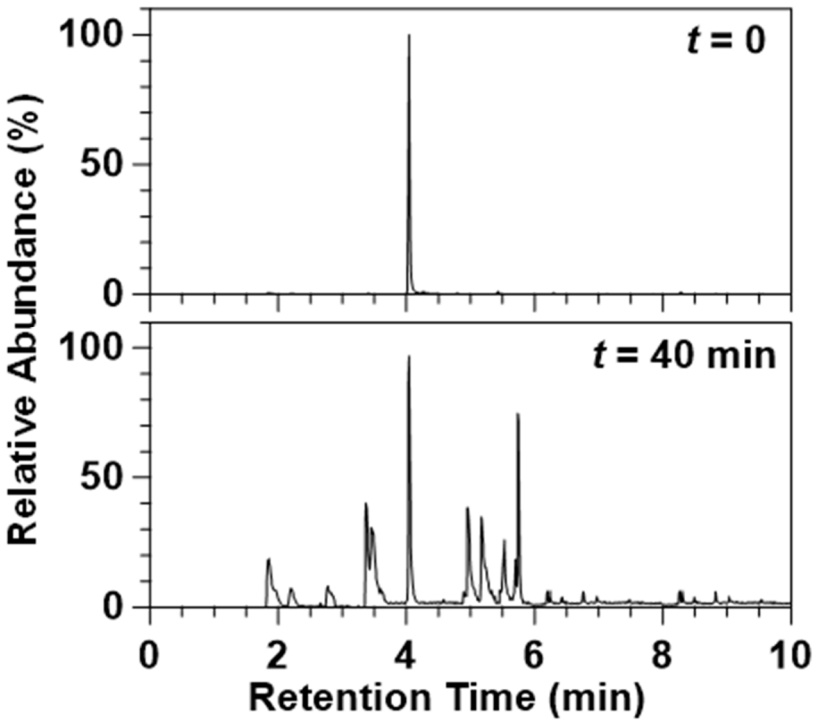

Figure S6. Chromatograms obtained for a 2MP and Cl_2 mixture (a) before irradiation and (b) after 40 min of irradiation.

At a retention time (RT) of 4.03 min, a strong peak can be observed corresponding to 2MP according to its mass spectrum. The rest of the peaks that appeared in the chromatogram were assigned to the following products using their mass spectra: acetaldehyde (RT = 1.95 min), butanedial (RT = 2.20 min), acetic acid (RT = 2.76 min), 2-pentanone (RT = 3.37 min), 3-pentanone (RT = 3.47 min), butanal (RT = 4.96 min), 2-methylbutanoic acid (RT = 5.55 min).

Other small peaks in the chromatogram were due to the degradation of the SPME fibre and the chromatographic column. Mass spectra of 2MP and the identified products are shown in **Figure S7**.

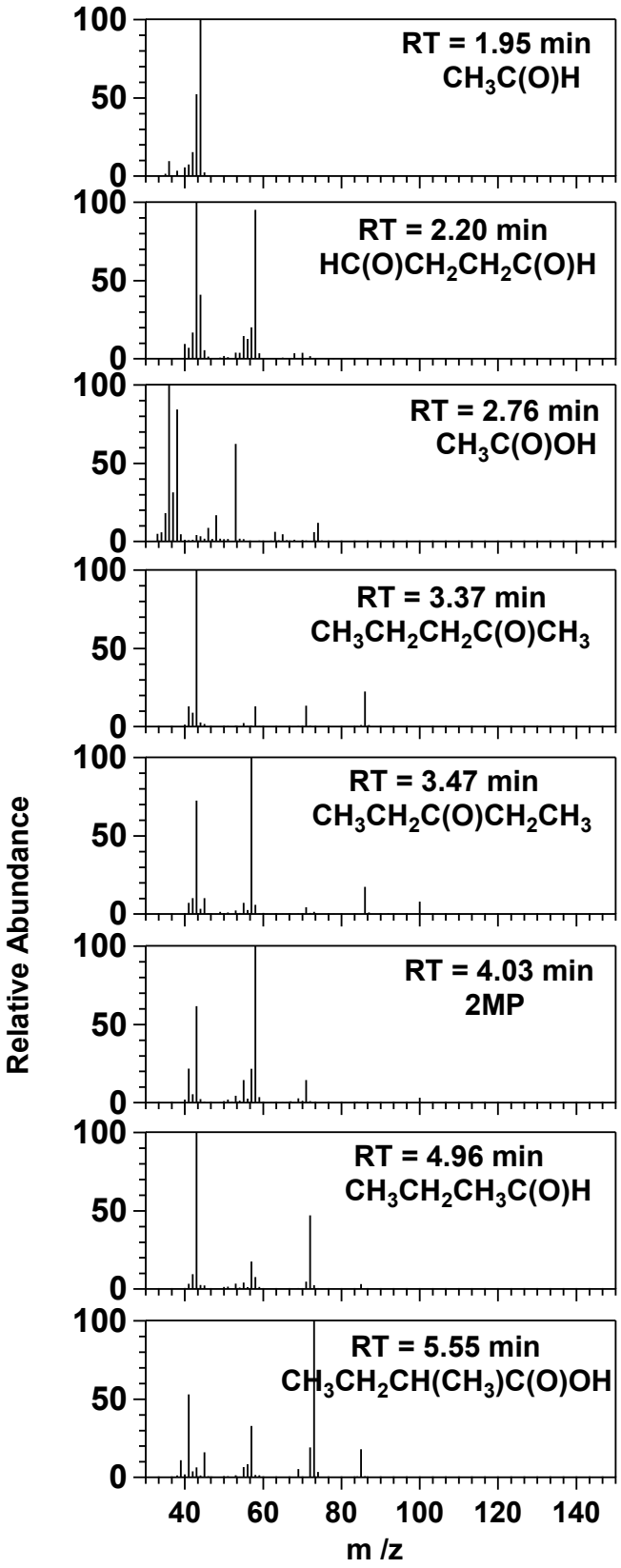

Figure S7. Mass spectra detected for the peaks of the chromatogram shown in Figure S6.

Detection by FTIR: In **Figure S8,** the FTIR spectra of a mixture of 2MP and Cl_2 in synthetic air before (initial) and after 15 min of the photolysis (with the features of 2MP subtracted) are shown. By comparison with the reference spectra (Figure S4), the major products were found to be CO, HCl, 2-pentanone, and acetaldehyde.

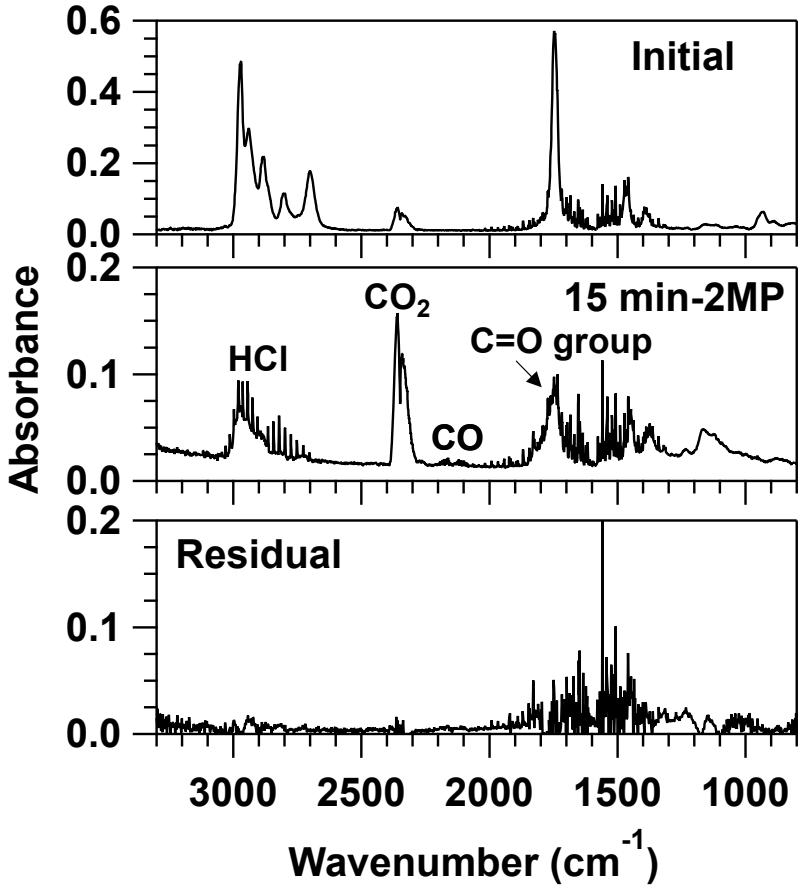

Figure S8. IR spectrum before irradiation (top), after 15 min of the Cl+2MP reaction with the 2MP features subtracted (middle) and the residual spectrum after subtraction of the IR features of the identified products (bottom).

The molar yield of a product, Y_{Product}, is defined as:

$$Y_{\text{Product}} = \frac{[\text{Product}]}{\Delta[\text{2MP}]} \qquad \text{(ES5)}$$

The concentration of a product, [Product], was corrected considering its loss by Cl reaction. Product concentrations were corrected to account for their Cl-reaction loss as explained by Ceacero-Vega et al. (2012). Plots of [Product] versus Δ[2MP] showed a linear behaviour for all these products, indicating that they are primary products (see Figure S9).

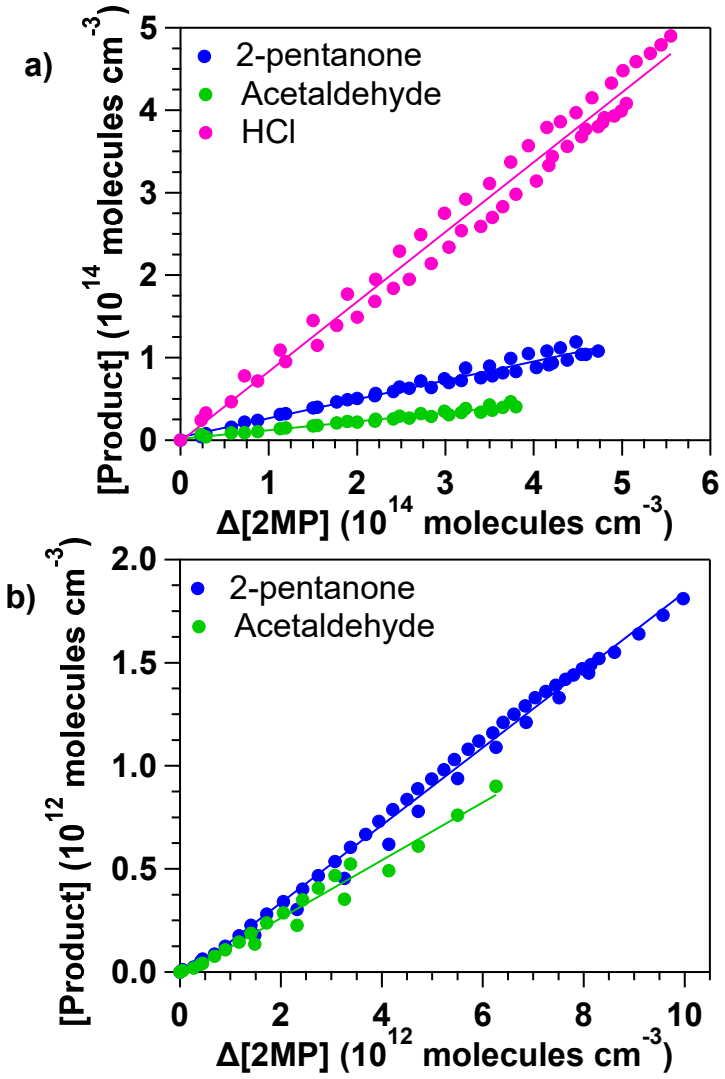

Figure S9. Plots to obtain the product yields of reaction R2 determined by a) FTIR spectroscopy and b) PTR-ToF-MS.

Note that during the test exposure to UV light of 2MP small amounts of 2-pentanone, acetaldehyde, and CO ($<7\times10^{12}$ molecule cm^{-3}) were detected and negligible compared with the observed in the Cl reaction ($>1\times10^{14}$ molecule cm^{-3}). The [CO] versus Δ[2MP] plot was curved in most of its range, what indicates that CO is mostly a secondary product. For that reason, no CO yields are provided in this work. CO_2 was not quantified since it is a final product of different reaction pathways. The minor products identified were 2-methylbutanoic acid, acetic acid, and formaldehyde. The yield plots for these products were curved from the beginning, so molar yields have not been calculated for these products.

Kinetics of the OH + 2MP reaction as a function of temperature.

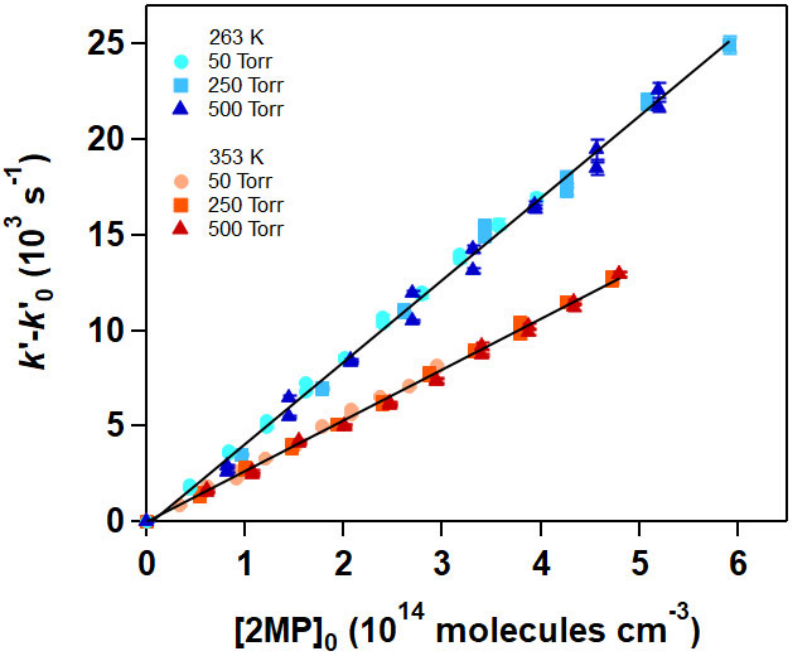

Figure S10. Examples of the $k'–k'_0$ *vs* $[2MP]_0$ plots (Eq. ES3) at 263 and 353 K in the 50-500 Torr pressure range.

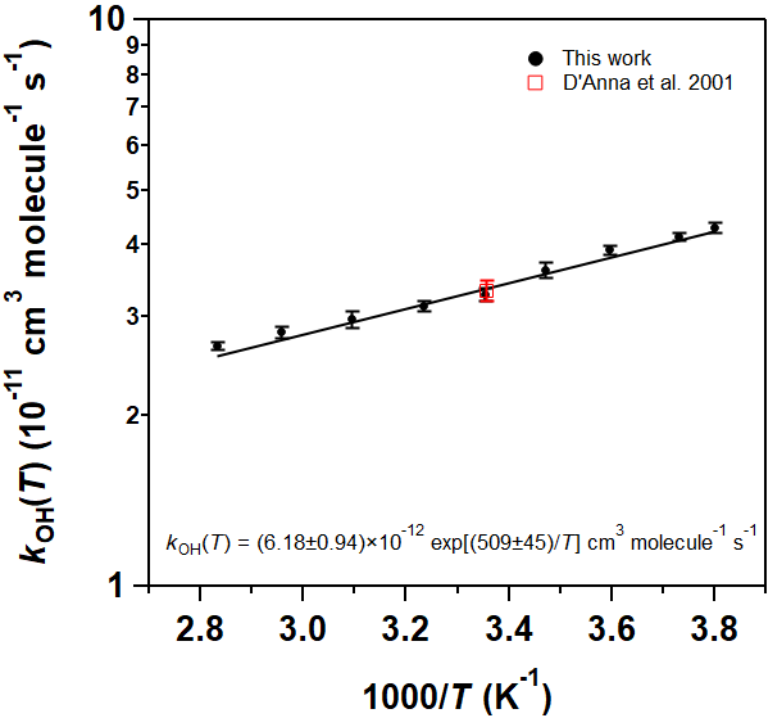

Figure S11. Plot of the temperature dependence of rate coefficient between 2MP and OH radicals, and Arrhenius fit, together with the literature value reported by D'Anna et al. (2001). Quoted error bars corresponds to ±2σ statistical errors.

Table S5. Individual rate coefficients and results from combing all kinetic data (±2σ) for the OH + 2MP reaction as a function of total pressure and temperature.

T / K	P_T / Torr	$k_{OH}(T)$ / 10^{-11} cm^3 molecule^{-1} s^{-1}	T / K	P_T / Torr	$k_{OH}(T)$ / 10^{-11} cm^3 molecule^{-1} s^{-1}
263	50	4.36 ± 0.10	309	50	3.16 ± 0.12
	50	4.34 ± 0.08		50	3.12 ± 0.09
	250	4.32 ± 0.12		**50**	3.12 ± 0.07
	250	4.31 ± 0.23	323	50	2.93 ± 0.12
	500	4.34 ± 0.15		50	2.97 ± 0.13
	500	4.21 ± 0.14		**50**	**2.96 ± 0.10**
	50-500	**4.29 ± 0.08**	338	50	2.80 ± 0.05
268	50	4.13 ± 0.06		50	2.84 ± 0.10
	50	4.15 ± 0.12		**50**	**2.82 ± 0.07**
	50	**4.15 ± 0.07**	353	50	2.73 ± 0.09
278	50	3.95 ± 0.08		50	2.73 ± 0.07
	50	3.91 ± 0.11		250	2.68 ± 0.07
	50	**3.93 ± 0.07**		250	2.70 ± 0.05
288	50	3.56 ± 0.16		500	2.68 ± 0.09
	50	3.62 ± 0.14		500	2.64 ± 0.10
	50	3.60 ± 0.11		**50-500**	**2.66 ± 0.04**
298	50	3.39 ± 0.14			
	50	3.41 ± 0.09			
	250	3.29 ± 0.21			
	250	3.38 ± 0.13			
	500	3.12 ± 0.09			
	500	3.21 ± 0.16			
	50-500	**3.28 ± 0.08**			

Photolysis lifetime of 2MP

245

Table S6. Estimated photolysis rate coefficients for 2MP.

Scenario	Season	Time (GMT + 1)	z/ km	θ/ º	$J(z,\theta)$/ s^{-1}
i	Winter	13:00	0.6	62.27	1.35×10^{-5}
	Summer	13:00	0.6	16.00	3.60×10^{-5}
ii	Winter	08:30	0.0	88.15	4.04×10^{-7}
	Summer	07:00	0.0	76.00	3.77×10^{-6}

References

Antiñolo, M., Asensio, M., Albaladejo, J., and Jiménez, E.: Gas-Phase Reaction of trans-2-Methyl-2-butenal with Cl: Kinetics, Gaseous Products, and SOA Formation, Atmosphere, 11, 715, https://doi.org/10.3390/atmos11070715, 2020.

Antiñolo, M., Olmo, R. d., Bravo, I., Albaladejo, J., and Jiménez, E.: Tropospheric fate of allyl cyanide (CH_2=$CHCH_2CN$): Kinetics, reaction products and secondary organic aerosol formation, Atmospheric Environment, 219, 117041, https://doi.org/10.1016/j.atmosenv.2019.117041, 2019.

Asensio, M., Antiñolo, M., Blázquez, S., Albaladejo, J., and Jiménez, E.: Evaluation of the daytime tropospheric loss of 2-methylbutanal, Atmospheric Chemistry and Physics, 22, 2689-2701, https://doi.org/10.5194/acp-22-2689-2022, 2022.

Ballesteros, B., Jiménez, E., Moreno, A., Soto, A., Antiñolo, M., and Albaladejo, J.: Atmospheric fate of hydrofluoroolefins, $C_xF_{2x+1}CH$=CH_2 (x = 1,2,3,4 and 6): Kinetics with Cl atoms and products, Chemosphere, 167, 330-343, https://doi.org/10.1016/j.chemosphere.2016.09.156, 2017.

Ceacero-Vega, A. A., Ballesteros, B., Bejan, I., Barnes, I., Jiménez, E., and Albaladejo, J.: Kinetics and Mechanisms of the Tropospheric Reactions of Menthol, Borneol, Fenchol, Camphor, and Fenchone with Hydroxyl Radicals (OH) and Chlorine Atoms (Cl), The Journal of Physical Chemistry A, 116, 4097-4107, https://doi.org/10.1021/jp212076g, 2012.

D'Anna, B., Andresen, Ø., Gefen, Z., and Nielsen, C. J.: Kinetic study of OH and NO_3 radical reactions with 14 aliphatic aldehydes, Physical Chemistry Chemical Physics, 3, 3057-3063, https://doi.org/10.1039/B103623H, 2001.

Gueymard, C. A., Myers, D., and Emery, K.: Proposed reference irradiance spectra for solar energy systems testing, Solar Energy, 73, 443-467, https://doi.org/10.1016/S0038-092X(03)00005-7, 2002.